
P3O: Policy-on Policy-off Policy Optimization

Rasool Fakoore*
Amazon Web Services

Pratik Chaudhari
Amazon Web Services

Alexander J. Smola
Amazon Web Services

Abstract

On-policy reinforcement learning (RL) algorithms have high sample complexity while off-policy algorithms are difficult to tune. Merging the two holds the promise to develop efficient algorithms that generalize across diverse environments. It is however challenging in practice to find suitable hyper-parameters that govern this trade off. This paper develops a simple algorithm named P3O that interleaves off-policy updates with on-policy updates. P3O uses the effective sample size between the behavior policy and the target policy to control how far they can be from each other and does not introduce any additional hyper-parameters. Extensive experiments on the Atari-2600 and MuJoCo benchmark suites show that this simple technique is effective in reducing the sample complexity of state-of-the-art algorithms. Code to reproduce experiments in this paper is at <https://github.com/rasoolfa/P3O>.

1 INTRODUCTION

Reinforcement Learning (RL) refers to techniques where an agent learns a policy that optimizes a given performance metric from a sequence of interactions with an environment. There are two main types of algorithms in reinforcement learning. In the first type, called on-policy algorithms, the agent draws a batch of data using its current policy. The second type, known as off-policy algorithms, reuse data from old policies to update the current policy. Off-policy algorithms such as Deep Q-Network (Mnih et al., 2015, 2013) and Deep Deterministic Policy Gradients DDPG (Lillicrap et al., 2015) are biased (Gu et al., 2017) because behavior of past policies

may be very different from that of the current policy and hence old data may not be a good candidate to inform updates of the current policy. Therefore, although off-policy algorithms are data efficient, the bias makes them unstable and difficult to tune (Fujimoto et al., 2018). On-policy algorithms do not usually incur a bias¹; they are typically easier to tune (Schulman et al., 2017) with the caveat that since they look at each data sample only once, they have poor sample efficiency. Further, they tend to have high variance gradient estimates which necessitates a large number of online samples and highly distributed training (Ilyas et al., 2018; Mnih et al., 2016).

Efforts to combine the ease-of-use of on-policy algorithms with the sample efficiency of off-policy algorithms have been fruitful (Gu et al., 2016; O’Donoghue et al., 2016b; Wang et al., 2016; Gu et al., 2017; Nachum et al., 2017; Degris et al., 2012). These algorithms merge on-policy and off-policy updates to trade-off the variance of the former against the bias of the latter. Implementing these algorithms in practice is however challenging: RL algorithms already have a lot of hyper-parameters (Henderson et al., 2018) and such a combination further exacerbates this. This paper seeks to improve the state of affairs.

We introduce the Policy-on Policy-off Policy Optimization (P3O) algorithm in this paper. It performs gradient ascent using the gradient

$$\begin{aligned} & \mathbb{E}_{\substack{s \sim d^{\pi_\theta} \\ a \sim \pi_\theta}} \left[\nabla \log \pi_\theta \hat{A}^{\pi_\theta} \right] + \mathbb{E}_{\substack{s \sim d^\beta \\ a \sim \beta}} \left[\min(\rho, c) \hat{A}^{\pi_\theta} \nabla \log \pi_\theta \right] \\ & - \lambda \nabla_\theta \mathbb{E}_{s \sim d^\beta, a \sim \beta} \text{KL} \left(\beta(\cdot|s) \parallel \pi_\theta(\cdot|s) \right) \end{aligned} \quad (1)$$

where the first term is the on-policy policy gradient, the second term is the off-policy policy gradient corrected by

¹Implementations of RL algorithms typically use the undiscounted state distribution instead of discounted distribution, which results in a bias. However, as Thomas (2014) show, being unbiased is not necessarily good and may even hurt performance.

Correspondence to: Rasool Fakoore [fakoore@amazon.com] and Pratik Chaudhari [prtic@amazon.com].

an importance sampling (IS) ratio ρ and the third term is a constraint that keeps the state distribution of the target policy π_θ close to that of the behavior policy β . Our key contributions are:

1. we automatically tune the IS clipping threshold c and the KL regularization coefficient λ using the normalized effective sample size (ESS), and
2. we control changes to the target policy using samples from replay buffer via an explicit Kullback-Leibler constraint.

The normalized ESS measures how efficient off-policy data is to estimate the on-policy gradient. We set

$$\lambda = 1 - \text{ESS} \quad \text{and} \quad c = \text{ESS}.$$

We show in Section 4 that this simple technique leads to consistently improved performance over competitive baselines on discrete action tasks from the Atari-2600 benchmark suite (Bellemare et al., 2013) and continuous action tasks from MuJoCo benchmark (Todorov et al., 2012).

2 BACKGROUND

Consider a discrete-time agent that interacts with the environment. The agent picks an action $a \in \mathcal{A}$ given the current state $s \in \mathcal{S}$ using a policy $\pi(a|s)$. It receives a reward $r(s, a) \in \mathbb{R}$ after this interaction and its objective is to maximize the discounted sum of rewards $G_t = \sum_{i=t}^{\infty} \gamma^{i-t} r(s_i, a_i)$ where $\gamma \in [0, 1)$ is a scalar constant that discounts future rewards. The quantity G_t is called the return. We shorten $r(s_t, a_t)$ to r_t to simplify notation.

If the initial state s_0 is drawn from a distribution $d^0(s)$ and the agent follows the policy π thereafter, the action-value function and the state-only value function are

$$\begin{aligned} q^\pi(s_t, a_t) &= \mathbb{E}_{(s,a) \sim \pi} [G_t | s_t, a_t], \quad \text{and} \\ v^\pi(s_t) &= \mathbb{E}_{a_t} [q^\pi(s_t, a_t)] \end{aligned} \quad (2)$$

respectively. The best policy $\pi^* = \arg \max_\pi J(\pi)$ maximizes the expected value of the returns where

$$J(\pi) = \mathbb{E}_{s \sim d^0} [v^\pi(s)]. \quad (3)$$

2.1 POLICY GRADIENTS

We denote by π_θ , a policy that is parameterized by parameters $\theta \in \mathbb{R}^n$. This induces a parameterization of the state-action and state-only value functions which we denote by q^{π_θ} and v^{π_θ} respectively. Monte-Carlo policy

gradient methods such as REINFORCE (Williams, 1992) solve for the best policy π_θ^* , typically using first-order optimization, using the likelihood-ratio trick to compute the gradient of the objective. Such a policy gradient of (3) is given by

$$\mathbb{E}_{s_t \sim d^{\pi_\theta}, a_t \sim \pi_\theta} [q^{\pi_\theta}(s_t, a_t) \nabla_\theta \log \pi_\theta(a_t | s_t)] \quad (4)$$

where d^{π_θ} is the unnormalized discounted state visitation frequency $d^{\pi_\theta}(s) = \sum_{t=0}^{\infty} \gamma^t \mathbb{P}(s_t = s)$.

Remark 1 (Variance reduction). The integrand in (4) is estimated in a Monte-Carlo fashion using sample trajectories drawn using the current policy π_θ . The action-value function q^{π_θ} is typically replaced by $\hat{q}^{\pi_\theta}(s_t, a_t) = \sum_{i=0}^{\infty} \gamma^i r_{t+i}$. Both of these approximations entail a large variance for policy gradients (Kakade and Langford, 2002; Baxter and Bartlett, 2001) and a number of techniques exist to mitigate the variance. The most common one is to subtract a state-dependent control variate (baseline) $\hat{v}^{\pi_\theta}(s)$ from $\hat{q}^{\pi_\theta}(s)$. This leads to the Monte-Carlo estimate of the advantage function (Konda and Tsitsiklis, 2000)

$$\hat{A}^{\pi_\theta}(s, a) = \hat{q}^{\pi_\theta}(s, a) - \hat{v}^{\pi_\theta}(s)$$

which is used in place of q^{π_θ} in (4). Let us note that more general state-action dependent baselines can also be used (Liu et al., 2017). We denote the baseline policy gradient integrand in short by $g(\pi_\theta) = \hat{A}^{\pi_\theta}(s, a) \nabla_\theta \log \pi_\theta(a|s)$ to rewrite (4) as

$$\nabla_\theta^{\text{on}} J(\pi_\theta) = \mathbb{E}_{s \sim d^{\pi_\theta}, a \sim \pi_\theta} [g(\pi_\theta)]. \quad (5)$$

2.2 OFF-POLICY POLICY GRADIENT

The expression in (5) is an expectation over data collected from the current policy π_θ . Vanilla policy gradient methods use each datum only once to update the policy which makes then sample inefficient. A solution to this problem is to use an experience replay buffer (Lin, 1992) to store previous data and reuse these experiences to update the current policy using importance sampling. For a mini-batch of size T consisting of $\{(s_k, a_k, s'_k)\}$ with $k \leq T$, the integrand in (5) becomes

$$\left(\prod_{t=0}^T \rho(s_t, a_t) \right) \sum_{t=0}^T \left(\sum_{i=0}^{T-t} \gamma^i r_{t+i} \right) \nabla_\theta \log \pi_\theta(a_t | s_t)$$

where the importance sampling (IS) ratio

$$\rho(s, a) = \frac{\pi_\theta(a|s)}{\beta(a|s)} > 0 \quad (6)$$

governs the relative probability of the candidate policy π_θ with respect to β .

Degrís et al. (2012) employed marginal value functions to approximate the above gradient and they obtained the expression

$$\mathbb{E}_{s \sim d^\beta, a \sim \beta} \left[\rho(s, a) \hat{A}^{\pi_\theta}(s, a) \nabla_\theta \log \pi_\theta(a|s) \right] \quad (7)$$

for the off-policy policy gradient. Note that states are sampled from d^β which is the discounted state distribution of β . Further, the expectation occurs using the policy β while the action-value function q^{π_θ} is that of the target policy π_θ . This is important because in order to use the off-policy policy gradient above, one still needs to estimate q^{π_θ} . The authors in Wang et al. (2016) estimate q^{π_θ} using the Retrace(λ) estimator (Munos et al., 2016). If π_θ and β are very different from each other (i) the importance ratio $\rho(s, a)$ may vary across a large magnitude, and (ii) the estimate of q^{π_θ} may be erroneous. This leads to difficulties in estimating the off-policy policy gradient in practice. An effective way to mitigate (i) is to clip $\rho(s, a)$ at some threshold c . We will use this clipped importance ratio often and denote it as $\bar{\rho}_c = \min(\rho, c)$. This helps us shorten the notation for the off-policy policy gradient to

$$\nabla_\theta^{\text{off}} J(\pi_\theta) = \mathbb{E}_{s \sim d^\beta, a \sim \beta} \left[\bar{\rho}_c g(\pi_\theta) \right]. \quad (8)$$

2.3 COVARIATE SHIFT

Consider the supervised learning where we observe iid data from a distribution $q(x)$, say the training dataset. We would however like to minimize the loss on data from another distribution $p(x)$, say the test data. This amounts to minimizing

$$\begin{aligned} & \mathbb{E}_{x \sim p(x)} \mathbb{E}_{y|x} [\ell(y, \varphi(x))] \\ &= \mathbb{E}_{x \sim q(x)} \mathbb{E}_{y|x} [w(x) \ell(y, \varphi(x))]. \end{aligned} \quad (9)$$

Here y are the labels associated to draws $x \sim q(x)$ and $\ell(y, \varphi(x))$ is the loss of the predictor $\varphi(x)$. The importance ratio is

$$w(x) := \frac{dp(x)}{dq(x)} \quad (10)$$

is the Radon-Nikodym derivative of the two densities (Resnick, 2013) and it re-balances the data to put more weight on unlikely samples in $q(x)$ that are likely under the test data $p(x)$. If the two distributions are the same, the importance ratio is 1 and this is unnecessary. When the two distributions are not the same, we have an instance of covariate shift and need to use the trick in (9).

Definition 2 (Effective sample size). Given a dataset $X = \{x_1, x_2, \dots, x_N\}$ and two densities $p(x)$ and $q(x)$ with $p(x)$ being absolutely continuous with respect to $q(x)$, the effective sample size is defined as the number of

samples from $p(x)$ that would provide an estimator with a performance equal to that of the importance sampling (IS) estimator in (9) with N samples (Kong, 1992). For our purposes, we will use the normalized effective sample size

$$\text{ESS} = \frac{1}{N} \|w(X)\|_1^2 / \|w(X)\|_2^2 \quad (11)$$

where $w(X) := [dp(x_1)/dq(x_1), \dots, dp(x_N)/dq(x_N)]$ is a vector that consists of evaluated at the samples. This expression is a good rule of thumb and is occurs, for instance, for a weighted average of Gaussian random variables (Quionero-Candela et al., 2009) or in particle filtering (Smith, 2013). We have normalized the ESS by the size of the dataset which makes $\text{ESS} \in [0, 1]$.

Note that estimating the importance ratio $w(x)$ requires the knowledge of both $p(x)$ and $q(x)$. While this is not usually the case in machine learning, reinforcement learning allows us access to both off-policy data and the on-policy data easily. We can therefore estimate $w(x)$ easily in RL. We can use the ESS as an indicator of the efficacy of updates to π_θ with samples drawn from the behavior policy β . If the ESS is large, the two policies predict similar actions given the state and we can confidently use data from β to update π_θ .

3 APPROACH

This section discusses the P3O algorithm. We first identify key characteristics of merging off-policy and on-policy updates and then discuss the details of the algorithm and provide insight into its behavior using ablation experiments.

3.1 COMBINING ON-POLICY AND OFF-POLICY GRADIENTS

We can combine the on-policy update (5) with the off-policy update (8) after bias-correction on the former as

$$\mathbb{E}_{\substack{s \sim d^{\pi_\theta} \\ a \sim \pi_\theta}} \left[\left(1 - \frac{c}{\rho}\right)_+ g(\pi_\theta) \right] + \mathbb{E}_{\substack{s \sim d^\beta \\ a \sim \beta}} \left[\bar{\rho}_c g(\pi_\theta) \right], \quad (12)$$

where $(\cdot)_+ := \max(\cdot, 0)$. This is similar to the off-policy actor-critic (Degrís et al., 2012) and ACER gradient (Wang et al., 2016) except that the authors in Wang et al. (2016) use the Retrace(λ) estimator to estimate q^{π_θ} in (8). The expectation in the second term is computed over actions that were sampled by β whereas the expectation of the first term is computed over all actions $a \in \mathcal{A}$ weighted by the probability of taking them $\pi_\theta(a|s)$. The clipping constant c in (12) controls the off-policy updates versus on-policy updates. As $c \rightarrow \infty$, ACER does a completely off-policy update while we have a completely on-policy update as $c \rightarrow 0$. In practice, it is difficult

to pick a value for c that works well for different environments as we elaborate upon in the following remark. This difficulty in choosing c is a major motivation for the present paper.

Remark 3 (How much on-policy updates does ACER do?). We would like to study the fraction of weight updates coming from on-policy data as compared to those coming from off-policy data in (12). We took a standard implementation of ACER² with published hyper-parameters from the original authors ($c = 10$) and plot the on-policy part of the loss (first term in (12)) as training progresses in Fig. 1. The on-policy loss is zero throughout training. This suggests that the performance of ACER (Wang et al., 2016) should be attributed predominantly to off-policy updates and the Retrace(λ) estimator rather than the combination of off-policy and on-policy updates. This experiment demonstrates the importance of hyper-parameters when combining off-policy and on-policy updates, it is difficult tune hyper-parameters that combine the two and work in practice.

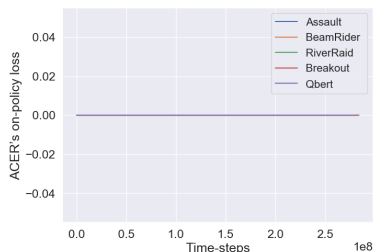


Figure 1: **On-policy loss for ACER is zero all through training due to aggressive importance ratio thresholding.** ACER had the highest reward from among A2C, PPO and P3O in 3 out of these 5 games (Assault, RiverRaid and BreakOut; see the Supplementary Material for more details). In spite of the on-policy loss being zero for all Atari games, ACER receives good rewards across the benchmark.

3.2 COMBINING ON-POLICY AND OFF-POLICY DATA WITH CONTROL VARIATES

Another way to leverage off-policy data is to use it to learn a control variate, typically the action-value function q_ω . This has been the subject of a number papers; recent ones include Q-Prop (Gu et al., 2016) which combines Bellman updates with policy gradients and Interpolated Policy Gradients (IPG) (Gu et al., 2017) which directly interpolates between on-policy and off-policy deterministic gradient, DPG and DDPG algorithms, (Silver et al., 2014; Lillicrap et al., 2016)) using a hyper-parameter. To

contrast with the ACER gradient in (12), the IPG is

$$(1-\nu) \mathbb{E}_{\substack{s \sim d^{\pi_\theta}, \\ a \sim \pi_\theta}} [g(\pi_\theta)] + \nu \nabla_\theta \mathbb{E}_{\substack{s \sim d^\beta, \\ a \sim \pi_\theta(a|s)}} [q_\omega(s, a)] \quad (13)$$

where q_ω is an off-policy fitted critic. Notice that since the policy π_θ is stochastic the above expression uses $\nabla_\theta \mathbb{E}_{a \sim \pi_\theta} \{q_\omega\}$ for the off-policy part instead of the DPG $\nabla_\theta q_\omega(s, \mu_\theta(s))$ for a deterministic policy $\mu_\theta(s)$. This avoids training a separate deterministic policy (unlike Q-Prop) for the off-policy part and encourages on-policy exploration and an implicit trust region update. The parameter ν explicitly controls the trade-off between the bias and the variance of off-policy and on-policy gradients respectively. However, we have found that it is difficult to pick this parameter in practice; this is also seen in the results of (Gu et al., 2017) which show sub-par performance on MuJoCo (Todorov et al., 2012) benchmarks; for instance compare these results to similar experiments in Fujimoto et al. (2018) for the Twin Delayed DDPG (TD3) algorithm.

3.3 P3O: POLICY-ON POLICY-OFF POLICY OPTIMIZATION

Our proposed approach, named Policy-on Policy-off Policy Optimization (P3O) explicitly controls the deviation of the target policy from the behavior policy. The gradient of P3O is given by

$$\begin{aligned} & \mathbb{E}_{s \sim d^{\pi_\theta}, a \sim \pi_\theta} [g(\pi_\theta)] + \mathbb{E}_{s \sim d^\beta, a \sim \beta} [\bar{\rho}_c g(\pi_\theta)] \\ & - \lambda \nabla_\theta \mathbb{E}_{s \sim d^\beta, a \sim \beta} \text{KL}(\beta(\cdot|s) \parallel \pi_\theta(\cdot|s)). \end{aligned} \quad (14)$$

The first term above is the standard on-policy gradient. The second term is the off-policy policy gradient with truncation of the IS ratio using a constant c while the third term allows explicit control of the deviation of the target policy π_θ from β . We do not perform bias correction in the first term so it is missing the factor $(1 - \frac{c}{\rho})_+$ from the ACER gradient (12). As we noted in Remark 3, it may be difficult to pick a value of c which keeps this factor non-zero. Even if the KL-term is zero, the above gradient is a biased estimate of the on-policy policy gradient. Further, the KL-divergence term can be rewritten as $\mathbb{E}_{s \sim d^\beta, a \sim \beta} [\log \rho]$ and therefore minimizes the importance ratio ρ over the entire replay buffer β . There are two hyper-parameters in the P3O gradient: the IS ratio threshold c and the KL regularization co-efficient λ . We use the following reasoning to pick them.

If the behavior and target policies are far from each other, we would like the λ be large so as to push them closer. If they are too similar to each other, it entails that we could

²OpenAI baselines: <https://github.com/openai/baselines>

have performed more exploration, in this scenario, we desire a smaller regularization co-efficient λ . We set

$$\lambda = 1 - \text{ESS} \quad (15)$$

where the ESS in (11) is computed using the current mini-batch sampled from the replay buffer β .

The truncation threshold c is chosen to keep the variance of the second term small. Smaller the c , less efficient the off-policy update and larger the c higher the variance of this update. We set

$$c = \text{ESS}. \quad (16)$$

This is a very natural way to threshold the IS factor $\rho(s, a)$ because $\text{ESS} \in [0, 1]$. This ensures an adaptive trade-off between the reduced variance of the gradient estimate and the inefficiency of a small IS ratio ρ . Note that the ESS is computed on a mini-batch of transitions and their respective IS factors and hence clipping an individual $\rho(s, a)$ using the ESS tunes c automatically to the mini-batch.

The gradient of P3O in (14) is motivated by the following observation: explicitly controlling the KL-divergence between the target and the behavior policy encourages them to have the same visitation frequencies. This is elaborated upon by Lemma 4 which follows from the time-dependent state distribution bound proved in (Schulman et al., 2015a; Kahn et al., 2017).

Lemma 4 (Gap in discounted state distributions). *The gap between the discounted state distributions d^{π_θ} and d^β is bounded as*

$$\|d^{\pi_\theta} - d^\beta\|_1 \leq \frac{2\gamma}{(1-\gamma)^2} \sqrt{\max_{s \in \mathcal{S}} \text{KL}(\beta \parallel \pi_\theta)} \quad (17)$$

The KL-divergence penalty in (14) is directly motivated from the above lemma; we however use $\mathbb{E}_{s \sim d^\beta, a \sim \beta} [\text{KL}(\pi_\theta \parallel \beta)]$ which is easier to estimate.

Remark 5 (Effect of λ). Fig. 2 shows the effect of picking a good value for λ on the training performance. We picked two games in Atari for this experiment: BeamRider which is an easy exploration task and Qbert which is a hard exploration task (Bellemare et al., 2016). As the figure and the adjoining caption shows, picking the correct value of λ is critical to achieving good sample complexity. The ideal λ also changes as the training progress because policies are highly entropic at initialization which makes exploration easier. It is difficult to tune λ using annealing schedules, this has also been mentioned by the authors in Schulman et al. (2017) in a similar context. Our choice of $\lambda = 1 - \text{ESS}$ adapts the level of regularization automatically.

Remark 6 (P3O adapts the bias in policy gradients). There are two sources of bias in the P3O gradient. First,

we do not perform correction of the on-policy term in (12). Second, the KL term further modifies the descent direction by averaging the target policy’s entropy over the replay buffer. If $\rho(s, a) > c$ for all transitions in the replay buffer, the bias in the P3O update is

$$\begin{aligned} & \mathbb{E}_{\substack{s \sim d^{\pi_\theta} \\ a \sim \pi_\theta}} \left[-\frac{c}{\rho} \hat{A}^{\pi_\theta} \nabla \log \pi_\theta \right] + \mathbb{E}_{s \sim d^\beta, a \in \mathcal{A}} \left[\lambda \nabla \log \pi_\theta(a|s) \right] \\ &= \mathbb{E}_{s \sim d^\beta, a \sim \beta} \left[-\text{ESS} \hat{A}^{\pi_\theta} \nabla \log \pi_\theta \right] \\ & \quad + \mathbb{E}_{s \sim d^\beta, a \in \mathcal{A}} \left[(1 - \text{ESS}) \nabla \log \pi_\theta(a|s) \right] \quad (18) \end{aligned}$$

The above expression suggests a very useful feature. If the ESS is close to 1, i.e., if the target policy is close to the behavior policy, P3O is a heavily biased gradient with no entropic regularization. On the other hand, if the ESS is zero, the entire expression above evaluates to zero. The choice $c = \text{ESS}$ therefore tunes the bias in the P3O updates adaptively. Roughly speaking, if the target policy is close to the behavior policy, the algorithm is confident and moves on even with a large bias. It is difficult to control the bias coming from the behavior policy, the ESS allows us to do so naturally.

A number of implementations of RL algorithms such as Q-Prop and IPG often have subtle, unintentional biases (Tucker et al., 2018). However, the improved performance of these algorithms, as also that of P3O, suggests that biased policy gradients might be a fruitful direction for further investigation.

3.4 DISCUSSION ON THE KL PENALTY

The KL-divergence penalty in P3O is reminiscent of trust-region methods. These are a popular way of making monotonic improvements to the policy and avoiding premature moves, e.g., see the TRPO algorithm by Schulman et al. (2015a). The theory in TRPO suggests optimizing a surrogate objective where the hard KL divergence constraint is replaced by a penalty in the objective. In our setting, this amounts to the penalty $\lambda \mathbb{E}_{s \sim \beta} [\text{KL}(\beta \parallel \pi_\theta)]$. Note that the behavior policy β is a mixture of previous policies and this therefore amounts to a penalty that keeps π_θ close to *all* policies in the replay buffer β . This is also done by the authors in Wang et al. (2016) to stabilize the high variance of actor-critic methods.

A penalty with respect to *all* past policies slows down optimization. This can be seen abstractly as follows. For an optimization problem $x^* = \arg \min_x f(x)$, the gradient update $x^{k+1} = x^k - \alpha^k \nabla f(x^k)$ can be written as

$$x^{k+1} = \arg \min_y \left\{ \langle \nabla f(x), y \rangle + \frac{1}{2\alpha^k} \|y - x^k\|^2 \right\}$$

if the arg min is unique; here x^k is the iterate and α^k is

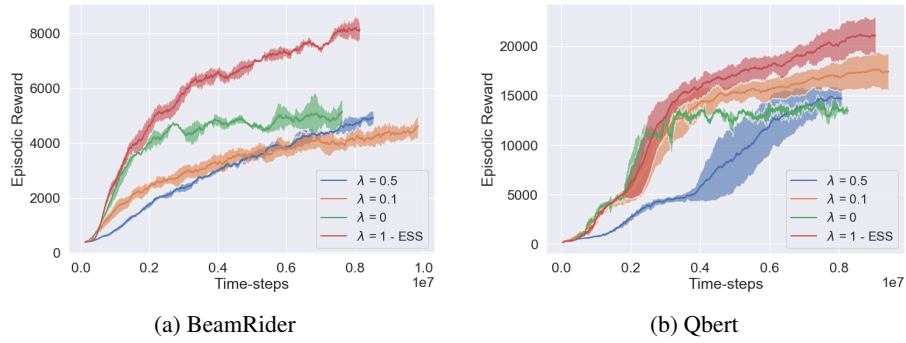


Figure 2: **Effect of λ on performance.** First, a non-zero value of λ trains much faster than without the KL regularization term because the target policy is constrained to be close to an entropic β . Second, for hard exploration games like Qbert, a smaller value $\lambda = 0.1$ works much better than $\lambda = 0.5$ while the trend is somewhat reversed for easy exploration games such as BeamRider. The ideal value of λ thus depends on the environment and is difficult to pick before-hand. Setting $\lambda = 1 - \text{ESS}$ tunes the regularization adaptively depending upon the particular mini-batch and works significantly better for easy exploration, it also leads to gains in hard exploration tasks.

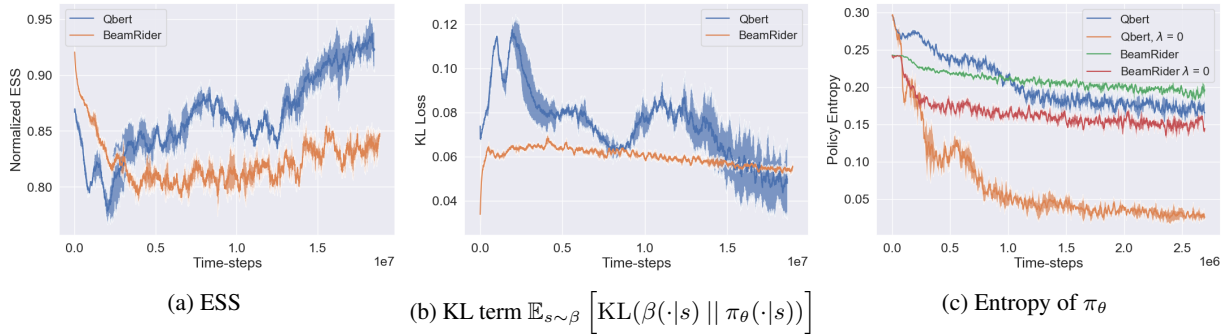


Figure 3: **Evolution of ESS, KL penalty and the entropy of π_θ as training progresses.** Fig. 3a shows the evolution of normalized ESS. A large value of ESS indicates that the target policy π_θ is close to β in its state distribution. The ESS is about 0.85 for a large fraction of the training which suggests a good trade-off between exploration and exploitation. The KL term in Fig. 3b is relatively constant during the course of training because its coefficient λ is adapted by ESS. This enables the target policy to be exploratory while still being able to leverage off-policy data from the behavior policy. Fig. 3c shows the evolution of the entropy of π_θ normalized by the number of actions $|\mathcal{A}|$. Note that using $\lambda = 0$ results in the target policy having a smaller entropy than standard P3O. This reduces its exploratory behavior and the latter indeed achieves a higher reward as seen in Fig. 2.

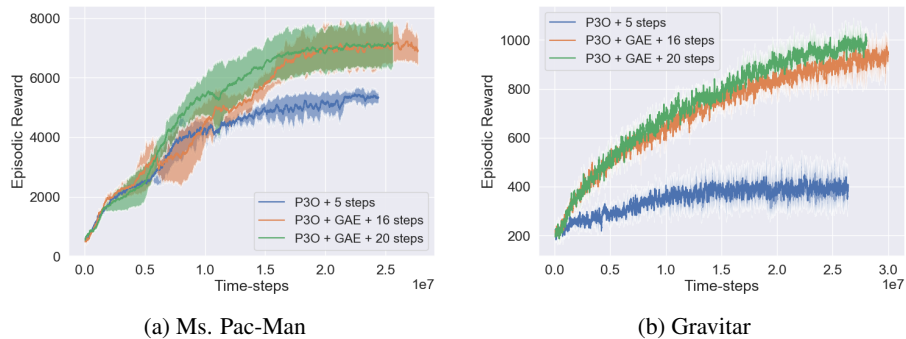


Figure 4: **Effect of roll-out length and GAE.** Figs. 4a and 4b show the progress of P3O with and without generalized advantage estimation. GAE leads to significant improvements in performance. The above figures also show the effect of changing the number of time-steps from the environment used in on-policy updates: longer time-horizons help in games with sparse rewards although the benefit diminishes across the suite after 20 steps.

the step-size at the k^{th} iteration. A penalty with respect to all previous iterates $\{x^1, x^2, \dots, x^k\}$ can be modeled as

$$x^{k+1} = \arg \min_y \left\{ \langle \nabla f(x), y \rangle + \frac{1}{2\alpha^k} \sum_{i=1}^k \|y - x^i\|^2 \right\} \quad (19)$$

which leads to the update equation

$$x^{k+1} = \frac{1}{k} \sum_{i=1}^k x^i - \frac{\alpha^k}{k} \nabla f(x^k)$$

which has a vanishing step-size as $k \rightarrow \infty$ if the schedule α^k is left unchanged. We would expect such a vanishing step-size of the policy updates to hurt performance.

The above observation is at odds with the performance of both ACER and P3O; see Section 4 which shows that both algorithms perform strongly on the Atari benchmark suite. However Fig. 3 helps reconcile this issue. As the target policy π_θ is trained, the entropy of the policy decreases, while older policies in the replay buffer are highly entropic and have more exploratory power. A penalty that keeps π_θ close to β encourages π_θ to explore. This exploration compensates for the decreased magnitude of the on-policy policy gradient seen in (19).

3.5 ALGORITHMIC DETAILS

The pseudo-code for P3O is given in Algorithm 1. At each iteration, it rolls out $K = 16$ trajectories of $T = 16$ time-steps each using the current policy and appends them to the replay buffer \mathcal{D} . In order to be able to compute the KL-divergence term, we store the policy $\pi_\theta(\cdot|s)$ in addition to the action for all states.

P3O performs sequential updates on the on-policy data and the off-policy data. In particular, Line 5 in Algorithm 1 samples a Poisson random variable that governs the number of off-policy updates for each on-policy update in P3O. This is also commonly done in the literature (Wang et al., 2016). We use Generalized Advantage Estimation (GAE) (Schulman et al., 2015b) to estimate the advantage function in P3O. We have noticed significantly improved results with GAE as compared to without it, as Fig. 4 shows.

4 EXPERIMENTAL VALIDATION

This section demonstrates empirically that P3O with the ESS-based hyper-parameter choices from Section 3 achieves, on-average, comparable performance to state-of-the-art algorithms. We evaluate the P3O algorithm against competitive baselines on the Atari-2600 benchmarks and MuJoCo continuous-control benchmarks.

Algorithm 1: One iteration of Policy-on Policy-off Policy Optimization (P3O)

Input: Policy π_θ , baseline v_ϕ , replay buffer \mathcal{D}

- 1 Roll out trajectories $\ell = \{\tau_1, \tau_2, \dots, \tau_K\}$ for T time-steps each
- 2 Compute the returns $G(\tau_k)$ and policy $\pi_\theta(\cdot|s_t; \tau_k)$ $\forall t \leq T, k \leq K$
- 3 $\mathcal{D} \leftarrow \mathcal{D} \cup \ell$
- 4 On-policy update of π_θ using ℓ ; see (14)
- 5 $\xi \leftarrow \text{Poisson}(m)$
- 6 **for** $i \leq \xi$ **do**
- 7 $\ell_i \leftarrow$ sample mini-batch from \mathcal{D}
- 8 Estimate ESS and KL-divergence term using π_θ and stored policies $\log \mu(\cdot|s_t; \tau_k) \forall t \leq T, \tau_k \in \ell_i$
- 9 Off-policy and KL regularizer update of π_θ using ℓ_i ; see (14)

4.1 SETUP

We compare P3O against three competitive baselines: the synchronous actor-critic architecture (A2C) Mnih et al. (2016), proximal policy optimization (PPO) Schulman et al. (2017) and actor-critic with experience replay (ACER) Wang et al. (2016). The first, A2C, is a standard baseline while PPO is a completely on-policy algorithm that is robust and has demonstrated good empirical performance. ACER combines on-policy updates with off-policy updates and is closest to P3O. We use the same network as that of Mnih et al. (2015) for the Atari-2600 benchmark and a two-layer fully-connected network for MuJoCo tasks. The hyper-parameters are the same as those of the original authors of the above papers in order to be consistent and comparable to existing literature. We use implementations from OpenAI Baselines³. We follow the evaluation protocol proposed by (Machado et al., 2017) and report the training returns for all experiments. More details are provided in the Supplementary Material.

4.2 RESULTS

Atari-2600 benchmark. Table 11 shows a comparison of P3O against the three baselines averaged over all the games in the Atari-2600 benchmark suite. We measure performance in two ways: (i) in terms of the final reward for each algorithm averaged over the last 100 episodes after 28M time-steps (112M frames of the game), and (ii) in terms of the reward at 40% training time and 80% training time averaged over 100 episodes. The latter compares different algorithms in terms of their sample efficiency. These results suggest that P3O is an efficient algorithm that improves upon competitive baselines both in terms of the final reward at the end of training and the reward

³<https://github.com/openai/baselines>

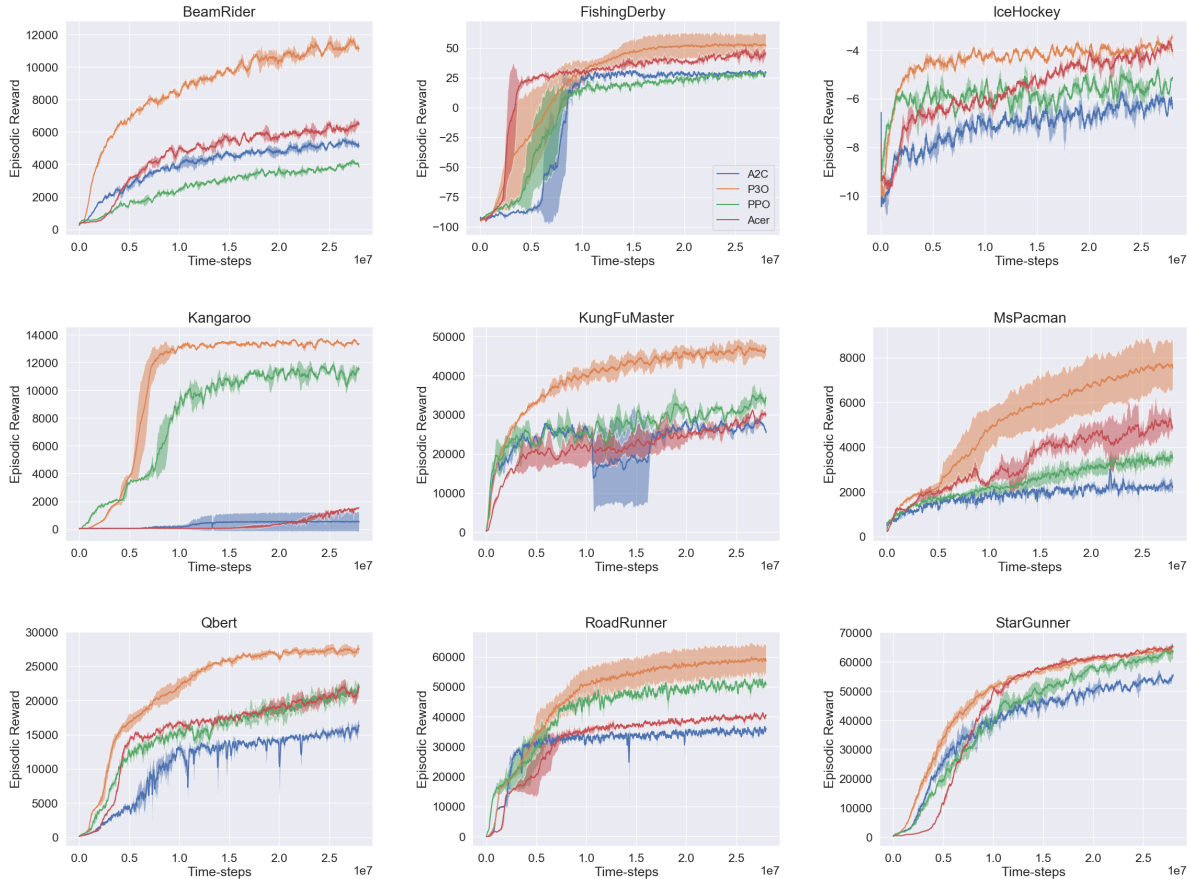


Figure 5: **Training curves for A2C (blue), ACER (red), PPO (green) and P3O (orange)** on some Atari games. See the Supplementary Material for similar plots on all Atari games.

obtained after a fixed number of samples. Fig. 7 shows the reward curves for some of games; rewards and training curves for all games are provided in the Supplementary Material.

Table 1: **Number of Atari games “won” by each algorithm** measured by the average return over 100 episodes across three random seeds.

Algorithm	Won	Won @ 40% training time	Won @ 80% training time
A2C	0	0	0
ACER	13	9	11
PPO	9	8	10
P3O	27	32	28

Completely off-policy algorithms are a strong benchmark on Atari games. We therefore compare P3O with a few state of the art off-policy algorithms using published results by the original authors. P3O wins 32 games vs. 17 games won by DDQN (Van Hasselt et al., 2016). P3O

wins 18 games vs. 30 games won by C51 (Bellemare et al., 2017). P3O wins 26 games vs. 22 games won by SIL (Oh et al., 2018). These off-policy algorithms use 200M frames and P3O’s performance with 112M frames is comparable to them.

MuJoCo continuous-control tasks. In addition to A2C and PPO, we also show a comparison to Q-Prop (Gu et al., 2016) and Interpolated Policy Gradients (IPG) (Gu et al., 2017); the returns for the latter are taken from the training curves in the original papers; they use 10M time-steps and 3 random seeds. The code of the original authors of ACER for MuJoCo is unavailable and we, as also others, were unsuccessful in getting ACER to train for continuous-control tasks. Table 2 shows that P3O achieves better performance than strong baselines for continuous-control tasks such as A2C and PPO. It is also better than on-average than algorithms such as Q-Prop and IPG designed to combine off-policy and on-policy data. Note that Q-Prop/IPG were tuned by the original authors specifically for each task. In contrast, all hyper-parameters for P3O are fixed across the Mu-

JoCo benchmarks. Training curves and results for more environments are in the Supplementary Material.

Table 2: **Average return on MuJoCo continuous-control tasks** after 3M time-steps of training on 10 seeds.

Task	A2C	PPO	Q-Prop	IPG	P3O
Half-Cheetah	1907	2022	4178	4216	5052
Walker	2015	2728	2832	1896	3771
Hopper	1708	2245	2957	-	2334
Ant	1811	1616	3374	3943	4727
Humanoid	720	530	1423	1651	2057

5 RELATED WORK

This work builds upon recent techniques that combine off-policy and on-policy updates in reinforcement learning. The closest to our approach is the ACER algorithm (Wang et al., 2016). It builds upon the off-policy actor-critic method (Degris et al., 2012) and uses the Retrace operator (Munos et al., 2016) to estimate an off-policy action-value function and constrains the candidate policy to be close to the running average of past policies using a linearized KL-divergence penalty. P3O uses a biased variant of the ACER gradient and incorporates an explicit KL penalty in the objective.

The PGQL algorithm (O’Donoghue et al., 2016a) uses an estimate of the action-value function of the target policy to combine on-policy updates with those obtained by minimizing the Bellman error. QProp (Gu et al., 2016) learns the action-value function using off-policy data which is used as a control variate for on-policy updates. The authors in Gu et al. (2017) propose the interpolated policy gradient (IPG) which takes a unified view of these algorithms. It directly combines on-policy and off-policy updates using a hyper-parameter and shows that, although such updates may be biased, the bias is bounded.

The key characteristic of the above algorithms is that they use hyper-parameters as a way to combine off-policy data with on-policy data. This is fragile in practice because different environments require different hyper-parameters. Moreover, the ideal hyper-parameters for combining data may change as training progresses; see Fig. 2. For instance, the authors in Oh et al. (2018) report poorer empirical results with ACER and prioritized replay as compared to vanilla actor-critic methods (A2C). The effective sample size heuristic (ESS) in P3O is a completely automatic, parameter-free way of combining off-policy data with on-policy data.

Policy gradient algorithms with off-policy data are not new. The importance sampling ratio has been commonly

used by a number of authors such as Cao (2005); Levine and Koltun (2013). Effective sample size is popularly used to measure the quality of importance sampling and to restrict the search space for parameter updates (Jie and Abbeel, 2010; Peshkin and Shelton, 2002). We exploit ESS to a similar end, it is an effective way to both control the contribution of the off-policy data and the deviation of the target policy from the behavior policy. Let us note there are a number of works that learn action-value functions using off-policy data, e.g., Wang et al. (2013); Hausknecht and Stone (2016); Lehnert and Precup (2015) that achieve varying degrees of success on reinforcement learning benchmarks.

Covariate shift and effective sample size have been studied extensively in the machine learning literature; see Robert and Casella (2013); Quionero-Candela et al. (2009) for an elaborate treatment. These ideas have also been employed in reinforcement learning (Kang et al., 2007; Bang and Robins, 2005; Dudík et al., 2011). To the best of our knowledge, this paper is the first to use ESS for combining on-policy updates with off-policy updates.

6 DISCUSSION

Sample complexity is the key inhibitor to translating the empirical performance of reinforcement learning algorithms from simulation to the real-world. Exploiting past, off-policy data to offset the high sample complexity of on-policy methods may be the key to doing so. Current approaches to combine the two using hyper-parameters are fragile. P3O is a simple, effective algorithm that uses the effective sample size (ESS) to automatically govern this combination. It demonstrates strong empirical performance across a variety of benchmarks. More generally, the discrepancy between the distribution of past data used to fit control variates and the data being gathered by the new policy lies at the heart of modern RL algorithms. The analysis of RL algorithms has not delved into this phenomenon. We believe this to be a promising avenue for future research.

7 ACKNOWLEDGEMENTS

The authors would like to acknowledge the support of Hang Zhang and Tong He from Amazon Web Services for the open-source implementation of P3O.

References

- Bang, H. and Robins, J. M. (2005). Doubly robust estimation in missing data and causal inference models. *Biometrics*, 61(4):962–973.
- Baxter, J. and Bartlett, P. L. (2001). Infinite-horizon policy-gradient estimation. *Journal of Artificial Intelligence Research*, 15:319–350.

- Bellemare, M., Srinivasan, S., Ostrovski, G., Schaul, T., Saxton, D., and Munos, R. (2016). Unifying count-based exploration and intrinsic motivation. In Lee, D. D., Sugiyama, M., Luxburg, U. V., Guyon, I., and Garnett, R., editors, *NIPS*, pages 1471–1479.
- Bellemare, M. G., Dabney, W., and Munos, R. (2017). A distributional perspective on reinforcement learning. In *Proceedings of the 34th International Conference on Machine Learning - Volume 70*, pages 449–458. JMLR. org.
- Bellemare, M. G., Naddaf, Y., Veness, J., and Bowling, M. (2013). The arcade learning environment: An evaluation platform for general agents. *Journal of Artificial Intelligence Research*, 47:253–279.
- Cao, X.-R. (2005). A basic formula for online policy gradient algorithms. *IEEE Transactions on Automatic Control*, 50(5):696–699.
- Degrís, T., White, M., and Sutton, R. S. (2012). Off-policy actor-critic. *arXiv:1205.4839*.
- Dudík, M., Langford, J., and Li, L. (2011). Doubly robust policy evaluation and learning. *arXiv:1103.4601*.
- Fujimoto, S., van Hoof, H., and Meger, D. (2018). Addressing function approximation error in actor-critic methods. *arXiv:1802.09477*.
- Gu, S., Lillicrap, T., Ghahramani, Z., Turner, R. E., and Levine, S. (2016). Q-prop: Sample-efficient policy gradient with an off-policy critic. *arXiv:1611.02247*.
- Gu, S. S., Lillicrap, T., Turner, R. E., Ghahramani, Z., Schölkopf, B., and Levine, S. (2017). Interpolated policy gradient: Merging on-policy and off-policy gradient estimation for deep reinforcement learning. In *NIPS*, pages 3846–3855.
- Hausknecht, M. and Stone, P. (2016). On-policy vs. off-policy updates for deep reinforcement learning. In *Deep Reinforcement Learning: Frontiers and Challenges, IJCAI 2016 Workshop*.
- Henderson, P., Islam, R., Bachman, P., Pineau, J., Precup, D., and Meger, D. (2018). Deep reinforcement learning that matters. In *Thirty-Second AAAI Conference on Artificial Intelligence*.
- Ilyas, A., Engstrom, L., Santurkar, S., Tsipras, D., Janoos, F., Rudolph, L., and Madry, A. (2018). Are deep policy gradient algorithms truly policy gradient algorithms? *arXiv:1811.02553*.
- Jie, T. and Abbeel, P. (2010). On a connection between importance sampling and the likelihood ratio policy gradient. In *Advances in Neural Information Processing Systems*, pages 1000–1008.
- Kahn, G., Zhang, T., Levine, S., and Abbeel, P. (2017). Plato: Policy learning using adaptive trajectory optimization. In *ICRA*, pages 3342–3349. IEEE.
- Kakade, S. and Langford, J. (2002). Approximately optimal approximate reinforcement learning. In *International Conference on Machine Learning*, volume 2, pages 267–274.
- Kang, J. D., Schafer, J. L., et al. (2007). Demystifying double robustness: A comparison of alternative strategies for estimating a population mean from incomplete data. *Statistical science*, 22(4):523–539.
- Konda, V. R. and Tsitsiklis, J. N. (2000). Actor-critic algorithms. In Solla, S. A., Leen, T. K., and Müller, K., editors, *NIPS*, pages 1008–1014. MIT Press.
- Kong, A. (1992). A note on importance sampling using standardized weights. *Technical Report 348*.
- Lehnert, L. and Precup, D. (2015). Policy gradient methods for off-policy control. *arXiv:1512.04105*.
- Levine, S. and Koltun, V. (2013). Guided policy search. In *International Conference on Machine Learning*, pages 1–9.
- Lillicrap, T. P., Hunt, J. J., Pritzel, A., Heess, N., Erez, T., Tassa, Y., Silver, D., and Wierstra, D. (2015). Continuous control with deep reinforcement learning. *arXiv:1509.02971*.
- Lillicrap, T. P., Hunt, J. J., Pritzel, A., Heess, N., Erez, T., Tassa, Y., Silver, D., and Wierstra, D. (2016). Continuous control with deep reinforcement learning. *CoRR*, abs/1509.02971.
- Lin, L.-J. (1992). Self-improving reactive agents based on reinforcement learning, planning and teaching. *Machine learning*, 8(3-4):293–321.
- Liu, H., Feng, Y., Mao, Y., Zhou, D., Peng, J., and Liu, Q. (2017). Action-dependent control variates for policy optimization via stein’s identity. *arXiv:1710.11198*.
- Machado, M. C., Bellemare, M. G., Talvitie, E., Veness, J., Hausknecht, M. J., and Bowling, M. (2017). Revisiting the arcade learning environment: Evaluation protocols and open problems for general agents. *CoRR*, abs/1709.06009.
- Mnih, V., Badia, A. P., Mirza, M., Graves, A., Lillicrap, T., Harley, T., Silver, D., and Kavukcuoglu, K. (2016). Asynchronous methods for deep reinforcement learning. In *ICML*, pages 1928–1937.
- Mnih, V., Kavukcuoglu, K., Silver, D., Graves, A., Antonoglou, I., Wierstra, D., and Riedmiller, M. (2013). Playing atari with deep reinforcement learning. *arXiv:1312.5602*.
- Mnih, V., Kavukcuoglu, K., Silver, D., Rusu, A. A., Veness, J., Bellemare, M. G., Graves, A., Riedmiller, M., Fidjeland, A. K., Ostrovski, G., et al. (2015). Human-level control through deep reinforcement learning. *Nature*, 518(7540):529.
- Munos, R., Stepleton, T., Harutyunyan, A., and Bellemare, M. (2016). Safe and efficient off-policy reinforcement learning. In *NIPS*, pages 1054–1062.
- Nachum, O., Norouzi, M., Xu, K., and Schuurmans, D. (2017). Bridging the gap between value and policy based reinforcement learning. In *NIPS*.
- O’Donoghue, B., Munos, R., Kavukcuoglu, K., and Mnih, V. (2016a). Combining policy gradient and q-learning. *arXiv:1611.01626*.
- O’Donoghue, B., Munos, R., Kavukcuoglu, K., and Mnih, V. (2016b). PGQ: Combining policy gradient and Q-learning. *arXiv:1611.01626*.
- Oh, J., Guo, Y., Singh, S., and Lee, H. (2018). Self-imitation learning. *arXiv:1806.05635*.
- Peshkin, L. and Shelton, C. R. (2002). Learning from scarce experience. *cs/0204043*.
- Quiñero-Candela, J., Sugiyama, M., Schwaighofer, A., and Lawrence, N. D. (2009). *Dataset shift in machine learning*. The MIT Press.
- Resnick, S. I. (2013). *A probability path*. Springer Science & Business Media.

- Robert, C. and Casella, G. (2013). *Monte Carlo statistical methods*. Springer Science & Business Media.
- Schulman, J., Levine, S., Abbeel, P., Jordan, M. I., and Moritz, P. (2015a). Trust region policy optimization. In *International Conference on Machine Learning*, volume 37, pages 1889–1897.
- Schulman, J., Moritz, P., Levine, S., Jordan, M., and Abbeel, P. (2015b). High-dimensional continuous control using generalized advantage estimation. *arXiv:1506.02438*.
- Schulman, J., Wolski, F., Dhariwal, P., Radford, A., and Klimov, O. (2017). Proximal policy optimization algorithms. *arXiv:1707.06347*.
- Silver, D., Lever, G., Heess, N., Degris, T., Wierstra, D., and Riedmiller, M. (2014). Deterministic policy gradient algorithms. In *International Conference on Machine Learning*.
- Smith, A. (2013). *Sequential Monte Carlo methods in practice*. Springer Science & Business Media.
- Thomas, P. (2014). Bias in natural actor-critic algorithms. In *Proceedings of the 31st International Conference on Machine Learning*, volume 32, pages 441–448. PMLR.
- Todorov, E., Erez, T., and Tassa, Y. (2012). Mujoco: A physics engine for model-based control. In *2012 IEEE/RSJ International Conference on Intelligent Robots and Systems*, pages 5026–5033. IEEE.
- Tucker, G., Bhupatiraju, S., Gu, S., Turner, R. E., Ghahramani, Z., and Levine, S. (2018). The mirage of action-dependent baselines in reinforcement learning. *arXiv:1802.10031*.
- Van Hasselt, H., Guez, A., and Silver, D. (2016). Deep reinforcement learning with double q-learning. In *Thirtieth AAAI Conference on Artificial Intelligence*.
- Wang, Y.-H., Li, T.-H. S., and Lin, C.-J. (2013). Backward q-learning: The combination of sarsa algorithm and q-learning. *Engineering Applications of Artificial Intelligence*, 26(9):2184–2193.
- Wang, Z., Bapst, V., Heess, N., Mnih, V., Munos, R., Kavukcuoglu, K., and de Freitas, N. (2016). Sample efficient actor-critic with experience replay. *arXiv:1611.01224*.
- Williams, R. J. (1992). Simple statistical gradient-following algorithms for connectionist reinforcement learning. *Machine Learning*, 8(3-4):229–256.

Appendix

A Hyper-parameters for all experiments

Table 3: **A2C hyper-parameters on Atari benchmark**

Hyper-parameters	Value
Architecture	conv (32-8 × 8-4) conv (64-4 × 4-2) conv (64-3 × 1-1) FC (512)
Learning rate	7×10^{-4}
Number of environments	16
Number of steps per iteration	5
Entropy regularization (α)	0.01
Discount factor (γ)	0.99
Value loss Coefficient	0.5
Gradient norm clipping coefficient	0.5
Random Seeds	{0...2}

Table 4: **ACER hyper-parameters on Atari benchmark**

Hyper-parameters	Value
Architecture	Same as A2C
Replay Buffer size	5×10^4
Learning rate	7×10^{-4}
Number of environments	16
Number of steps per iteration	20
Entropy regularization (α)	0.01
Number of training epochs per update	4
Discount factor (γ)	0.99
Value loss Coefficient	0.5
importance weight clipping factor	10
Gradient norm clipping coefficient	0.5
Momentum factor in the Polyak	0.99
Max. KL between old & updated policy	1
Use Trust region	True
Random Seeds	{0...2}

Table 5: **PPO hyper-parameters on Atari benchmark**

Hyper-parameters	Value
Architecture	Same as A2C
Learning rate	7×10^{-4}
Number of environments	8
Number of steps per iteration	128
Entropy regularization (α)	0.01
Number of training epochs per update	4
Discount factor (γ)	0.99
Value loss Coefficient	0.5
Gradient norm clipping coefficient	0.5
Advantage estimation discounting factor (τ)	0.95
Random Seeds	{0...2}

Table 6: **P3O hyper-parameters on Atari benchmark**

Hyper-parameters	Value
Architecture	Same as A2C
Learning rate	7×10^{-4}
Replay Buffer size	5×10^4
Number of environments	16
Number of steps per iteration	16
Entropy regularization (α)	0.01
Off policy updates per iteration (ξ)	Poisson(2)
Burn-in period	15×10^3
Samples from replay buffer	6
Discount factor (γ)	0.99
Value loss Coefficient	0.5
Gradient norm clipping coefficient	0.5
Advantage estimation discounting factor (τ)	0.95
Random Seeds	{0...2}

Table 7: **P3O hyper-parameters for MuJoCo tasks**

Hyper-parameters	Value
Architecture	FC(100) - FC(100)
Learning rate	3×10^{-4}
Replay Buffer size	5×10^3
Number of environments	2
Number of steps per iteration	64
Entropy regularization (α)	0.0
Off policy updates per iteration (ξ)	Poisson(3)
Burn-in period	2500
Number of samples from replay buffer	15
Discount factor (γ)	0.99
Value loss Coefficient	0.5
Gradient norm clipping coefficient	0.5
Advantage estimation discounting factor (τ)	0.95
Random Seeds	{0...9}

Table 8: **A2C (and A2C with GAE) hyper-parameters on MuJoCo tasks**

Hyper-parameters	Value
Architecture	FC(64) - FC(64)
Learning rate	13×10^{-3}
Number of environments	8
Number of steps per iteration	32
Entropy regularization (α)	0.0
Discount factor (γ)	0.99
Value loss Coefficient	0.5
Gradient norm clipping coefficient	0.5
Random Seeds	{0...9}

Table 9: PPO hyper-parameters on MuJoCo tasks

Hyper-parameters	Value
Architecture	FC(64) - FC(64)
Learning rate	3×10^{-4}
Number of environments	1
Number of steps per iteration	2048
Entropy regularization (α)	0.0
Number of training epochs per update	10
Discount factor (γ)	0.99
Value loss Coefficient	0.5
Gradient norm clipping coefficient	0.5
Advantage estimation discounting factor (τ)	0.95
Random Seeds	{0...9}

B Comparisons with baseline algorithms

Table 10: Returns on MuJoCo continuous-control tasks after 3M time-steps of training and 10 random seeds.

Games	A2CG	A2C	PPO	P3O
Half-Cheetah	181.46	1907.42	2022.14	5051.58
Walker	855.62	2015.15	2727.93	3770.86
Hopper	1377.07	1708.22	2245.03	2334.32
Swimmer	33.33	45.27	101.71	116.87
Inverted Double Pendulum	90.09	5510.71	4750.69	8114.05
Inverted Pendulum	733.34	889.61	414.49	985.14
Ant	-253.54	1811.29	1615.55	4727.34
Humanoid	530.12	720.38	530.13	2057.17

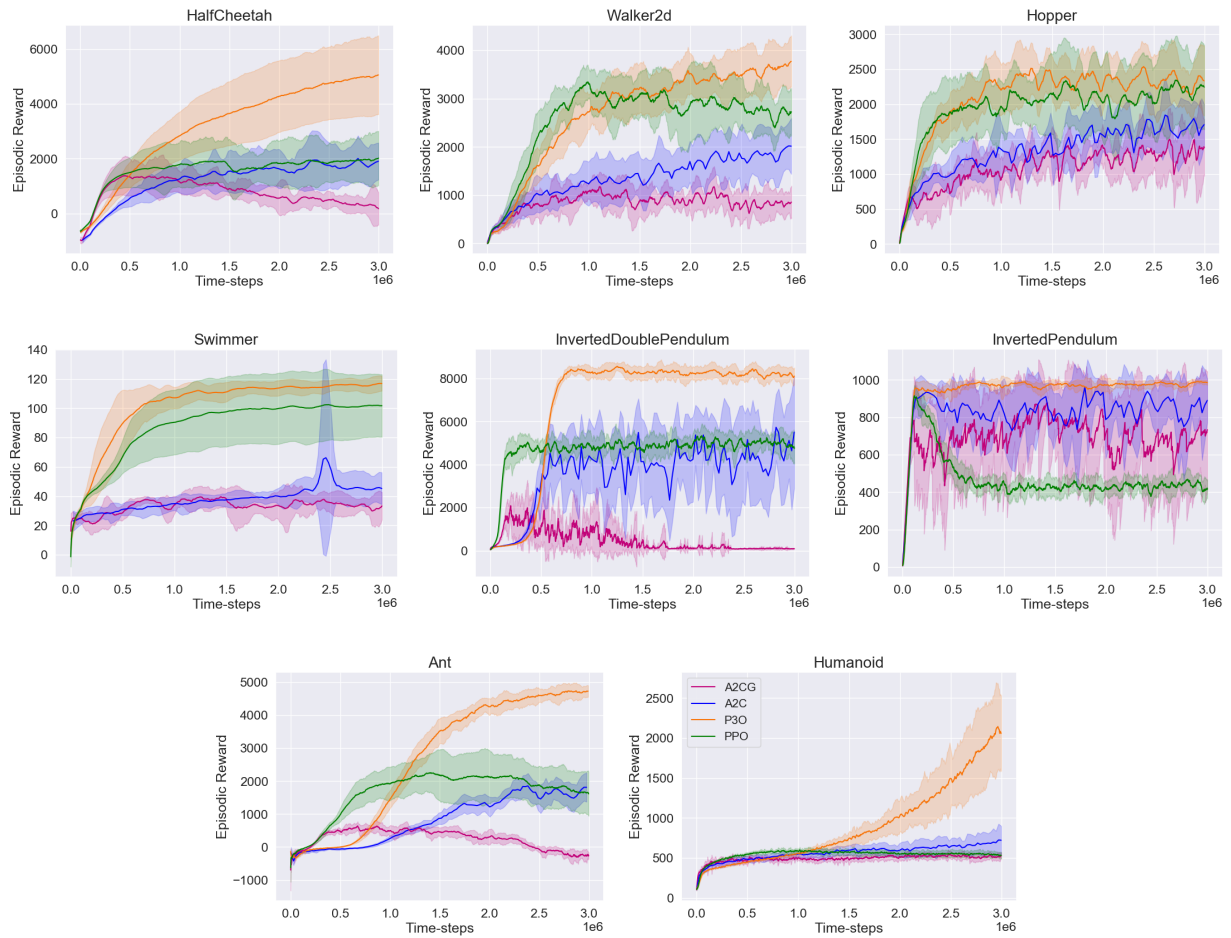


Figure 6: Training curves of A2C (blue), A2CG [A2C with GAE] (magenta), PPO (green) and P3O (orange) on 8 MuJoCo environments.

Table 11: Returns of agents on 49 Atari-2600 games after 28M timesteps (112M frames) of training.

Games	A2C	ACER	PPO	P3O
Alien	1425.00	2436.20	2260.43	3124.80
Amidar	439.43	1393.24	1062.73	1787.40
Assault	3897.73	6996.46	5941.23	6222.27
Asterix	12272.50	24414.00	7574.33	25997.00
Asteroids	2052.27	1874.83	2147.33	2483.30
Atlantis	2847251.67	2832752.33	2647593.67	3077883.00
BankHeist	910.43	1281.60	1236.90	864.03
BattleZone	6250.00	10726.67	22856.67	12793.33
BeamRider	5149.29	6486.07	3834.01	11163.49
Bowling	24.19	38.61	31.75	27.04
Boxing	0.21	99.33	98.06	99.44
Breakout	403.25	474.81	328.80	351.81
Centipede	3722.24	6755.41	4530.21	8615.36
ChopperCommand	1389.67	10376.00	9504.33	8878.33
CrazyClimber	111418.67	136527.67	118501.00	168115.00
DemonAttack	65766.90	181679.27	37026.17	331454.95
DoubleDunk	-17.86	-8.37	-6.29	-3.83
Enduro	0.00	0.00	1092.52	0.00
FishingDerby	29.54	45.74	29.34	52.07
Freeway	0.00	0.00	32.83	0.00
Frostbite	269.87	304.23	1266.73	312.13
Gopher	3923.13	99855.53	6451.07	29603.60
Gravitar	377.33	387.00	1042.67	987.50
IceHockey	-6.39	-3.97	-5.11	-3.50
Jamesbond	453.83	457.50	683.67	475.00
Kangaroo	507.33	1524.67	11583.67	13360.67
Krull	8935.40	9115.73	8718.40	7812.03
KungFuMaster	25395.00	30002.33	34292.00	46761.67
MontezumaRevenge	0.00	0.00	0.00	805.33
MsPacman	2220.63	4892.33	3502.20	7516.21
NameThisGame	5977.63	15640.83	6011.03	9232.70
Pitfall	-65.50	-7.64	-1.94	-7.40
Pong	20.21	20.80	20.69	20.95
PrivateEye	49.24	99.00	97.33	92.61
Qbert	16289.08	22051.67	21830.17	27619.33
Riverraid	9680.33	17794.03	11841.03	13966.67
RoadRunner	35918.33	40428.67	50663.33	58728.00
Robotank	4.30	4.89	18.54	33.69
Seaquest	1485.33	1739.87	1953.53	1851.87
SpaceInvaders	1894.02	3140.17	2124.57	2699.33
StarGunner	55469.33	65005.00	63375.67	63905.00
Tennis	-22.22	-11.26	-6.72	-5.27
TimePilot	3359.00	7012.00	7535.67	10789.00
Tutankham	105.28	291.09	206.42	268.24
UpNDown	30932.20	159642.17	173208.13	279107.53
Venture	0.00	0.00	0.00	0.00
VideoPinball	21061.76	373803.36	220680.47	377935.99
WizardOfWor	1256.33	2973.00	5744.67	10637.33
Zaxxon	17.00	89.33	8872.67	16801.33

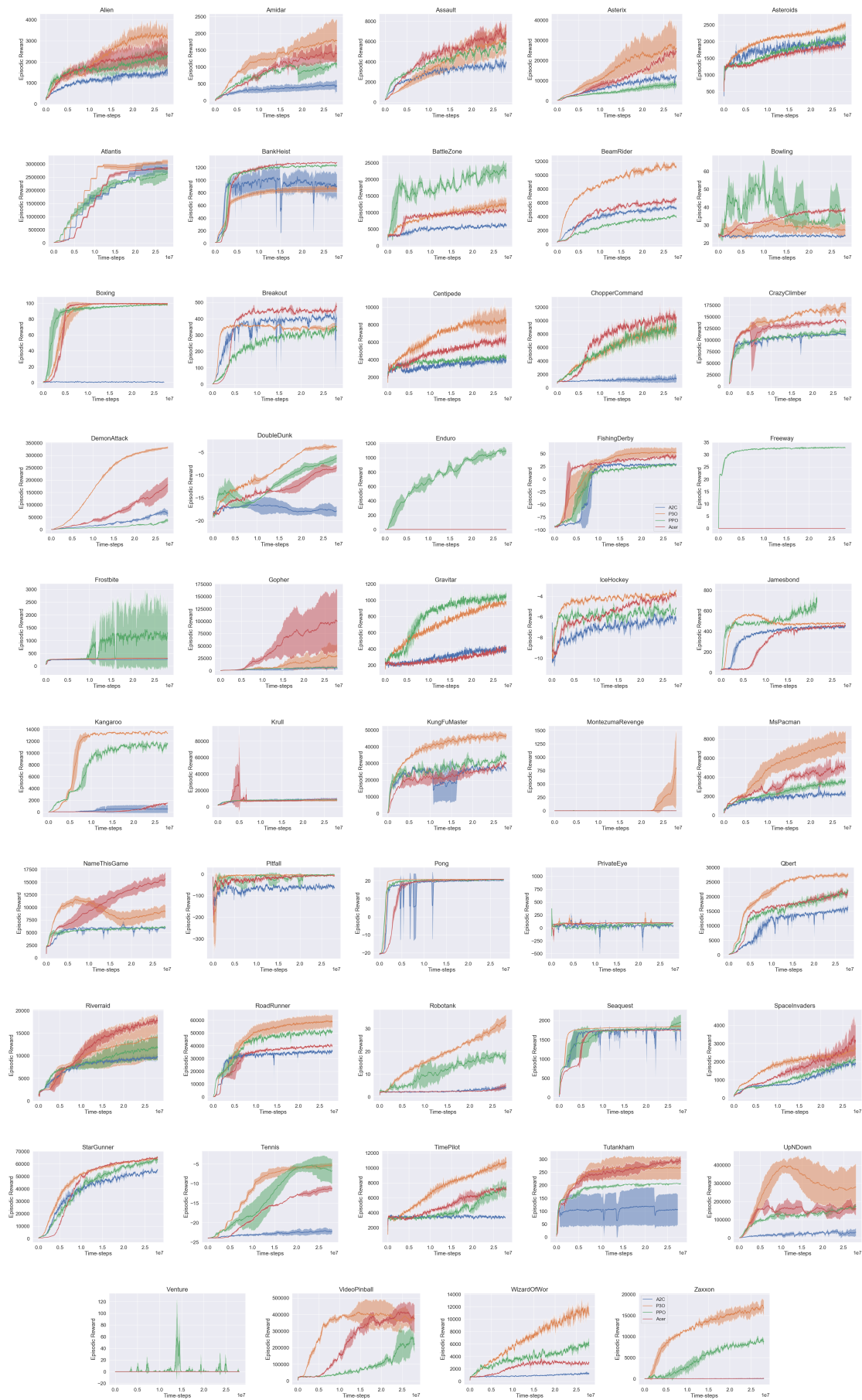


Figure 7: Training curves of A2C (blue), ACER (red), PPO (green) and P3O (orange) on all 49 Atari games.